PHYSICAL REVIEW B VOLUME 9, NUMBER 4 15 FEBRUARY 1974

Phonon dispersion and instability in linear-chain crystals

B. Horovitz and M. Weger
Nuclear Research Center, Negev, P.O.B. 9001, Beer-Sheva, Israel

H. Gutfreund
The Racah Institute of Physics, The Hebrew University, Jerusalem, Israel

(Received 27 August 1973)

This paper deals extensively with the coupling of phonons to an electron gas with a Fermi surface consisting of two parallel planes and its effect on the stability of the lattice and on the phonon dispersion around $2p_F$. The phonon dispersion and the phonon spectral density distributions are calculated at zero temperature for the equidistant and the deformed lattice, and at temperatures above the transition temperature to the deformed lattice. Two excitation branches are found under certain conditions. The calculation is performed in the random-phase approximation, but the effect of vertex renormalization by summing all ladder diagrams is discussed. The phonon dispersion in the distorted lattice is also treated within the framework of the Sawada model.

I. INTRODUCTION

In the recent years there has been a growing interest in the properties of materials with quasi-one-dimensional electronic systems. One class of such materials contains intermetallic compounds of the A-15 (β-tungsten) crystal structure.[1] There is a theoretical indication,[2,3] supported by experimental evidence,[4] that the Fermi surface of several of these compounds contains planar sections, reflecting the presence of groups of electrons, which are restricted to move in one dimension. This one-dimensional character is the basis of the Labbe-Friedel-Barisic model.[3,5] Another class of quasi-one-dimensional materials consists of organic conductors[6] like the tetracyanoquinodimethan (TCNQ) charge-transfer salts and the Krogman compounds (for example, $K_2Pt(CN)_4Br_{0.30}3H_2O$).

The present paper deals mainly with the effects of one dimensionality on the phonon spectrum. The coupling to a one-dimensional electron system affects the electrons in the neighborhood of $q = 0$ and $q = 2p_F$. The first region was investigated by Engelsberg and Varga[7] within the framework of the Tomonaga model. Although we shall briefly discuss these regions, our main purpose is to study the vicinity of $q = 2p_F$, where the Tomonaga model does not apply, since it excludes excitations across the Fermi surface and is valid only for long-wavelength phonons. We adopt an idealized picture of an electron gas with a Fermi surface consisting of two parallel planes separated by $2p_F$ and limited by the Brillouin-zone boundaries. Such a system was investigated by Alfanas'ev and Kagan,[8] who pointed out that in this case the phonon spectrum near $2p_F$ differs considerably from the case of a spherical Fermi surface. The origin of this effect is the sharp increase in the phase-space volume available for low-energy-electron excitations accompanied by the absorption or emission of phonons with $q \simeq 2p_F$. This leads to a strong coupling with such phonons and, thus, to a significant renormalization of the phonon spectrum in this region, which results in a much stronger Kohn singularity than for a spherical (three-dimensional) or cylindrical (two-dimensional) Fermi surface. The Kohn singularity in the one-dimensional case is a manifestation of the instability discussed by Peierls[9] and Fröhlich.[10]

After formulating the model in Sec. II, we discuss in Sec. III the phonon spectrum at $T = 0$. In the first part of this section we calculate, within the random-phase approximation (RPA), the phonon spectrum near $q = 0$ and reproduce the results of Ref. 7. We then consider the region $q \simeq 2p_F$, the main conclusion being the appearance of two phonon branches. The RPA is valid as long as Migdal's theorem, which asserts that the electron-phonon vertex may be approximated by the bare coupling constant, holds. This theorem breaks down in the one-dimensional case and a proper renormalization of the electron-phonon vertex is required. We perform such a renormalization in the last part of Sec. III by summing the "ladder" diagrams and discuss its effect on the phonon spectrum. Most of the results of this section were reported in a short communication.[11]

The nature of the instability resulting from the strong electron-phonon coupling is discussed in Sec. IV. The energy of the system is minimized by producing a stable lattice distortion of wave vector $q = 2p_F$, which leads to an energy gap in the single-electron excitations. This is the result of Fröhlich.[9] The phonon spectrum of the distorted lattice near $2p_F$ is also calculated. If the coupling is not too strong, so that the energy gap does not exceed the unperturbed frequency ω_0, one gets again two-phonon branches near $q = 2p_F$. The lower

undamped branch contains the point $\omega = 0$ at $q = 2p_F$. The phonon dispersion in the distorted lattice is treated again in the framework of the Sawada[12] model in Sec. V. This is a solvable model which generally reproduces the results of RPA. It is based on certain assumptions which can be checked *a posteriori* to justify the applicability of the model.

In Sec. VI we compute the phonon dispersion at finite temperatures. As long as the Peierls-Fröhlich instability temperature T_p is less than the bare-phonon energy, the phonon spectral density distribution exhibits a two-branch structure as the temperature is lowered and approaches T_p. Similar results were recently obtained by Barisic *et al.*[13] As T comes extremely close to T_p the mean-square deviation of the ions diverges because of critical vibrations of momentum $q = 2p_F$. This is discussed in Sec. VII.

The nature of the instability, the characteristics of the phonon dispersion, and the possible existence and properties of two-phonon branches are the underlying questions of the present work. They may be relevant to the understanding of three recent observations on, presumably, quasi-one-dimensional systems. One is the appearance of two narrow phonon-excitation peaks in the neutron-scattering experiments of Axe and Shirane[14] on Nb_3Sn. We believe at present that our simple treatment is inadequate to reproduce this result. This point is discussed in some detail in Sec. VIII. The second experimental result to which our work may bear some relevance is the suggestion by Coleman *et al.*[15] of strong paraconductivity above 60 °K in tetrathiofulvalinium (TTF)-TCNQ crystals. This was interpreted by the authors of Ref. 15 as BCS-pairing fluctuations and the high T_c was attributed to the soft phonons associated with the Peierls instability. This idea was further developed by the authors of the present paper.[16] A different interpretation was suggested by Bardeen,[17] who invoked Fröhlich's original idea[18] of a moving lattice distortion carrying along the electron "sea" through the crystal.

Although Bardeen's interpretation is probably correct, the question arises whether materials like TTF-TCNQ can *at all* be superconductors, and if so, whether the transition temperature may be high.[18-20] This question may depend critically on the nature of the phonon softening investigated in this work.

The third experimental result is the observation by neutron diffraction[21] of a possible Kohn anomaly in $K_2Pt(CN)_4Br_{0.3}3H_2O$ similar to the one investigated here.

II. MODEL

We start from the Fröhlich Hamiltonian

$$H=\sum_p \epsilon_p c_p^\dagger c_p+\sum_q \omega_q^0 a_q^\dagger a_q + \sum_{p,q} g_q (a_q + a_{-q}^\dagger)\, c_{p+q}^\dagger c_p \quad , \tag{2.1}$$

where c_p, a_q are the electron and phonon destruction operators and g_q is the electron-phonon coupling constant. We find it convenient to characterize the strength of this coupling by a dimensionless parameter s_q, defined by

$$g_q^2 = s_q \pi^3 \omega_q^0 / \beta m p_F \quad , \tag{2.2}$$

where m is the electron mass, p_F is the Fermi momentum, and $\beta = \int dp_x dp_y / p_F^2$. The parameter β is related to the electron density by $n = \frac{1}{2}\beta(p_F/\pi)^3$. The coupling constant may also be expressed by

$$g_q^2 = |\langle k+q \,|\, \nabla U \,|\, k\rangle|^2 / 2NM\omega_q^0 \tag{2.3}$$

(or, $\nabla\langle k+q\,|\,U\,|\,k\rangle$ instead of $\langle k+q\,|\,\nabla U\,|\,k\rangle$, following Barisic[5]), where N is the density of ions, M is their mass, and U is the electron-ion potential. One can use this form together with Eq. (2.2) to estimate s for $q = 2p_F$. Fermi-surface averages of the matrix elements in Eq. (2.3) for various materials were given by McMillan.[22] The value of p_F may be estimated from positron-annihilation measurements[4] and $\omega_{2p_F}^0$ from the Debye temperature or, for optical phonons, from the molecular vibration frequency. On the grounds of such crude estimates one gets for V_3Si, $s = 0.1-0.5$.

For the reader's convenience we relate our parameter s with the dimensionless parameters used by other authors to characterize the electron-phonon interaction: (a) $s \simeq 8/q$, for $s \lesssim 1$ (Barisic[5,13]), (b) $s = \frac{4}{3}F\nu$ (Frölich[10]) and (c) $s = \alpha^2/4$ (Engelsberg and Varga[7]). For $s \ll 1$, $s \approx 2\lambda$ (McMillan[22]).

We assume that the electron energies are given by $\epsilon_p = p^2/2m$, although the tight-binding form of ϵ_p seems to be more suitable for the materials under consideration. However, we are interested in drastic effects on the phonon spectrum, which are not sensitive to the detailed behavior of the electron dispersion.

All the information about the phonon spectrum is contained in the phonon Green's function

$$D(q,\omega) = 2\omega_q^0 / [\omega^2 - (\omega_q^0)^2 - 2\omega_q^0 \Pi(q,\omega)] \tag{2.4}$$

where $\Pi(q,\omega)$ is the phonon self-energy, given by

$$\Pi(q,\omega) = -[2i/(2\pi)^4] \int g_q \Gamma(p,\epsilon;q,\omega) \times G(p+q,\epsilon+\omega) G(p,\epsilon)\, d^3p\, d\epsilon \quad . \tag{2.5}$$

Γ is the electron-phonon vertex function. To close this set of equations, one has to add the equations for the electron Green's function G and the electron self-energy. We shall replace G by the free-electron Green's function G_0, the argument being that these two functions differ only in a small region of integration around the Fermi energy. However, more work is needed to verify this approximation. What is still needed is an approximation

for the vertex function. We shall replace Γ by the coupling constant g_q and solve for the poles of $D(q, \omega)$. The effect of higher-order corrections to Γ will be discussed in Sec. III C. These assumptions amount to the random-phase approximation for the phonon self-energy,

$$\Pi_0(q,\omega) = -[2i/(2\pi)^4] g_q^2 \int G_0(p+q, \epsilon+\omega) \times G_0(p,\epsilon)\, d^3p\, d\epsilon = -[2g_q^2/(2\pi)^3] \int d^3p \times \{(n_{p+q} - n_p)/[\omega - (\epsilon_{p+q} - \epsilon_p) + i\delta]\}, \ \delta = +0 \tag{2.6}$$

where n_p is the electron-momentum distribution. We have used here the retarded form of the "bubble" propagator,[23] which for $\omega > 0$ is identical to the Feynman propagator. Assuming that the integrand in Eq. (2.6) depends only on p_z (we drop the z index), using Eq. (2.2) and $\epsilon_p = p^2/2m$, we obtain after simple manipulations

$$\Pi_0(q,\omega) = -s_q \omega_q^0 I(q,\omega) \ , \tag{2.7}$$

where

$$I(q,\omega) = -\frac{p_F}{4q} \int_{-\infty}^{\infty} dp\, n_p \left(\frac{1}{p - m\omega/q - \frac{1}{2}q - i\delta} - \frac{1}{p - m\omega/q + \frac{1}{2}q - i\delta} \right) . \tag{2.8}$$

The phonon-excitation energies appear as poles of the function $D(q, \omega)$, or roots of the equation

$$\omega^2 = \omega_q^{0^2} [1 - 2s_q I(q,\omega)] \ . \tag{2.9}$$

III. PHONON DISPERSION AT $T = 0$

The momentum distribution at zero temperature is $n_p = \theta(\epsilon_F - \epsilon_p)$ [$\theta(x) = 1$ for $x > 0$, and $\theta(x) = 0$ for $x < 0$]. The integration in Eq. (2.8) is then straightforward and one obtains

$$\mathrm{Re} I(q,\omega) = \frac{p_F}{4q} \ln \left| \frac{(\frac{1}{2}q + p_F)^2 - (m\omega/q)^2}{(\frac{1}{2}q - p_F)^2 - (m\omega/q)^2} \right| \ , \tag{3.1}$$

$$\mathrm{Im} I(q,\omega) = (\pi p_F/4q) [\theta(|\tfrac{1}{2}q + m\omega/q| - p_F) - \theta(|\tfrac{1}{2}q - m\omega/q| - p_F)] \ . \tag{3.2}$$

It follows that $\mathrm{Im} I(q,\omega) \neq 0$ in the region (for $q > 0$)

$$v_F q\, |(q/2p_F) - 1| < \omega < v_F q (q/2p_F + 1) \ . \tag{3.3}$$

This is the region of possible electron-hole excitations of energy ω and momentum q, and it corresponds to the shaded area in Fig. 1. A phonon with q and ω in this region is expected to be attenuated, namely, its "dressed" energy is expected to be complex. The "bare" phonon-dispersion curve lies for most values of q much below the curve defined by the left-hand side of the inequality (3.3) as long as $v_F \gg v_s$. Barisic[5,13] assumes that k_F is very small, and v_F is not large compared with v_s. For this case, our approximations do not apply. It is therefore clear that the bare phonon frequencies for these values of q are almost unaffected by the electron-phonon interaction. The latter will be important only near $q = 0$ and $q = 2p_F$. Note that this is different from the case of a spherical Fermi surface where the shaded area extends down to the momentum axis between $q = 0$ and $q = 2p_F$, and the electron-phonon interaction is felt everywhere, but its effects are drastic nowhere.

A. Region $q \cong 0$

Let us now consider briefly what happens around $q = 0$. In the limit $q \to 0$, we get

$$I(q,\omega) = -\tfrac{1}{2}(v_F q)^2/[\omega^2 - (v_F q)^2] \tag{3.4}$$

and the phonon Green's function becomes

$$D(q,\omega) = \frac{2\omega_q^0}{\omega^2 - \omega_q^{0^2}[1 + s_q(v_F q)^2/\omega^2 - (v_F q)^2]} = 2\omega_q^0 \frac{\omega^2 - (v_F q)^2}{\omega_1^2 - \omega_2^2} \left(\frac{1}{\omega^2 - \omega_1^2} - \frac{1}{\omega^2 - \omega_2^2} \right) , \tag{3.5}$$

where ω_1 and ω_2 are two branches of dressed phonon excitations,

$$\omega_{1,2} = \tfrac{1}{2}\{\omega_q^{0^2} + (v_F q)^2 \pm [(\omega_q^{0^2} - (v_F q)^2)^2 + 4 s_q \omega_q^{0^2} (v_F q)^2]\}^{1/2} . \tag{3.6}$$

This is exactly the result obtained by Engelsberg and Varga[7] by solving the Tomonaga mode, which is not surprising since these authors showed that the Tomonaga model is equivalent to replacing the phonon self-energy Π by its expression in the RPA.

For an optical phonon ($\omega_q^0 = \omega_0$) we obtain, for $q \to 0$,

$$\omega_1^2 = \omega_0^2 + s_q (v_F q)^2 \ , \qquad \omega_2^2 = (v_F q)^2 (1 - s_q) . \tag{3.7}$$

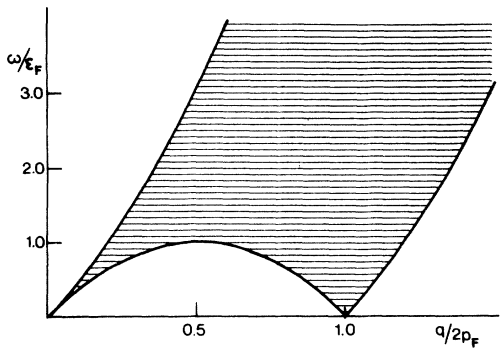

FIG. 1. Region of possible electron-hole excitation energies and momenta in a one-dimensional system (shaded area).

For an acoustic phonon ($\omega_q^0 = v_s q$), we get

$$\omega_1^2 = q^2(v_F^2 + s_q v_s^2)\,, \qquad \omega_2^2 = q^2 v_s^2(1 - s_q)\,. \tag{3.8}$$

These solutions lie outside the shaded area in Fig. 1 and are therefore real, as expected. By checking the residues of the two poles in $D(q, \omega)$, one finds that the weight of the higher branch falls off rapidly when q exceeds ω_q^0/v_F. As noticed by Wentzel,[24] the system becomes unstable when $s_q > 1$ for some small q.

B. Region $q \simeq 2p_F$

We shall now concentrate on the second region where the electron-phonon interaction is expected to be significant, namely, around $q = 2p_F$. Let us denote $q' = \frac{1}{2}q - p_F$ and consider $|q'| \ll p_F$. We are now looking for complex solutions of Eq. (2.9), and the function $I(q, \omega)$ has to be continued analytically to the complex ω plane. This is done by replacing ω by $\omega + i\gamma$ and subtracting for $\omega > 0$, $\gamma < 0$ the jump in the imaginary part across the real ω axis. Separating the real and imaginary parts of Eq. (2.9), we obtain for small q' the following two coupled equations for the real (ω) and imaginary (γ) parts of the phonon frequency,

$$\omega^2 - \gamma^2 = \omega_0^2 \times\left(1 + \tfrac{1}{8}s\,\ln\frac{[(\omega + 2v_F q')^2 + \gamma^2][(\omega - 2v_F q')^2 + \gamma^2]}{(8\epsilon_F)^4}\right) \tag{3.9}$$

$$2\omega\gamma = -\tfrac{1}{4}s\omega_0^2\left(\pi\theta(\omega - 2v_F|q'|) + \arctan\frac{2\omega\gamma}{(2v_F q')^2 + \gamma^2 - \omega^2}\right), \tag{3.10}$$

where $-\frac{1}{2}\pi \leq \arctan \leq \frac{1}{2}\pi$. We have assumed that s_q and ω_q^0 do not vary strongly in the neighborhood of $q = 2p_F$ and replaced them by constants s and ω_0. In view of the θ function, we consider separately the two possibilities: $\omega < 2v_F|q'|$ and $\omega > 2v_F|q'|$.

In the first case the only solution of Eq. (3.10) is $\omega\gamma = 0$ (due to the opposite signs on both sides). There exist two values q_1, q_2 ($0 < q_1 < 2p_F < q_2$), such that for $q_1 < q < q_2$ the solution is $\omega = 0$ and $\gamma \neq 0$ (actually γ may be of both signs), and $\omega \neq 0$, $\gamma = 0$ outside this region. For $s \lesssim 0.5$, the values of q_1, q_2 are very close to $2p_F$ and are given by

$$q_{1,2} \simeq 2p_F(1 \pm 2e^{-2/s})\,. \tag{3.11}$$

At the points q_1, q_2 themselves, $\omega = 0$ and $\gamma = 0$ is a solution of Eqs. (3.9) and (3.10). When s increases above 0.5, q_1 decreases rapidly until $q_1 = 0$ for $s = 1$. Thus for $s \geq 1$, there exist solutions with $\omega = 0$, $\gamma \neq 0$ in the entire range $0 < q < q_2$. Such solutions clearly indicate an instability of the system. In particular, a solution with $\omega = \gamma = 0$ reflects a static distortion of the lattice. This will be further discussed in the following sections. In general, when s_q depends on q, one gets an unstable solution for any q for which s_q exceeds a critical value $s_c(q)$. For this critical value $\omega = 0$, $\gamma = 0$ is a solution of Eqs. (3.9), (3.10), or Eq. (2.9), and it is therefore determined by the equation

$$1 = 2s_c(q)I(q, 0). \tag{3.12}$$

The parameter $s_c(q)$ for $T = 0$ is plotted in Fig. 6.

In the second case, when $\omega > 2v_F|q'|$, one finds a solution with $\omega \neq 0$, $\gamma \neq 0$, which exists as long as ω exceeds

$$v_F q\,|q/2p_F - 1| \simeq 2v_F|q'|\,.$$

This solution falls entirely within the shaded area in Fig. 1 and is therefore complex as expected. Both solutions are plotted for $s = 0.25$ and $\alpha = \omega_0/2\epsilon_F = 0.01$ in Fig. 2.

It is instructive to analyze the phonon dispersion with the help of the spectral density function, which is related to the phonon Green's function by

$$B(q, \omega)\,\mathrm{sgn}\omega = -(1/\pi)\,\mathrm{Im}D(q, \omega). \tag{3.13}$$

The function $B(q, \omega)$ measures the weight of the energy ω in the energy spread of phonon excitations of momentum q. It is defined on the real ω axis and reflects the existence of poles in the complex plane, if these are not too removed from the real axis. The solutions with $\omega \neq 0$ $\gamma = 0$ appear in $B(q, \omega)$ as δ functions. The solutions with $\omega = 0$, $\gamma \neq 0$, in the region $q_1 < q < q_2$, carry no spectral weight, since $B(q, \omega) = -B(q, -\omega)$, as long as B is continuous, and therefore $B(q, 0) = 0$. In the shaded region of Fig. 1, $B(q, \omega)$ is continuous and has a maximum at the solution with $\omega \neq 0$, $\gamma \neq 0$ (for $q \simeq 2p_F$). We shall further discuss the function $B(q, \omega)$ in subse-

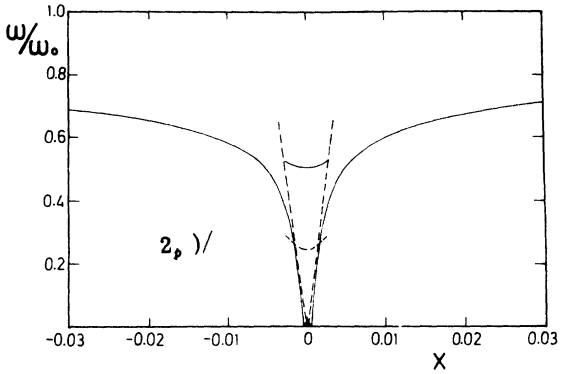

FIG. 2. Typical phonon dispersion curve at $T = 0$, near $q = 2p_F$, for $s = 0.25$ and $\alpha = \omega_0/2\epsilon_F = 0.01$. The broken lines correspond to $\omega = \pm 2v_F q'$. The broken curves are the negative imaginary parts of the damped solutions with $\omega \neq 0$ (the higher one) and with $\omega = 0$ (the small bump around $\omega = 0$, $q = 2p_F$). Momentum is measured in units of $x = (q - 2p_F)/2p_F$.

quent sections and show typical curves for the distorted lattice (Sec. IV) and finite temperatures (Sec. VI).

C. Effect of ladder diagrams

In Sec. III B we have replaced the electron-phonon vertex function by coupling constant g_q. This procedure is justified by Migdal's theorem which states that

$$\Gamma(p, \epsilon; p, \omega) \simeq g_q[1 + O(m/M)^{1/2}] \,. \tag{3.14}$$

In our case, however, already the lowest correction [Fig. 3(a)] to Γ has a logarithmic divergence[8] on the lines $\omega = \pm 2v_F|q'|$. One therefore should renormalize the electron-phonon vertex. The simplest renormalization is achieved by summing all the ladder diagrams [Fig. 3(b)]. In this approximation Γ satisfies the Dyson equation [Fig. 3(c)],

$$\begin{aligned}\Gamma(p, \epsilon; q, \omega) = g_q + [i/(2\pi)^4] \int d^3p' d\epsilon' \\ \times \Gamma(p', \epsilon': q, \omega) G_0(p' + q, \epsilon' + \omega) \\ \times G_0(p', \epsilon') g^2_{p-p'} D(p - p', \epsilon - \epsilon') \,,\end{aligned} \tag{3.15}$$

where D_0 is the unperturbed phonon Green's function. The dominant contribution to the integral over ϵ' comes from the region $\epsilon' \simeq \epsilon_{p'+q} - \omega \simeq \epsilon_{p'}$, because then the poles of the two Green's functions overlap. In the one-dimensional case this corresponds to $p' = -\frac{1}{2}q + m\omega/q$. Being interested in $q \simeq 2p_F$, we can neglect the second term because ω (energy of the incoming phonon) is much smaller than p_F^2/m. Thus, the main contribution to the integral in Eq. (3.15) comes from the neighborhood of $p' = -q/2$, $\epsilon' = \epsilon_{q/2}$. The factor $g^2 D_0$ does not vary significantly around this point and we take its value there outside the integral. We obtain, on account of Eq. (2.5),

$$\begin{aligned}\Gamma(p, \epsilon; q, \omega) = g_q - (1/2g_q) g^2_{p+q/2} g^2_{p+q/2} \\ \times D(p + \tfrac{1}{2}q, \epsilon - \epsilon_{q/2}) \Pi(q, \omega).\end{aligned} \tag{3.16}$$

Inserting this expression for Γ into Eq. (2.5), we get

$$\Pi(q, \omega) = \Pi_0(q, \omega) + \Pi(q, \omega) \tilde{I}(q, \omega), \tag{3.17}$$

where

$$\begin{aligned}\tilde{I}(q, \omega) = [i/(2\pi)^4] \int d^3k \, d\epsilon g_k^2 \\ \times D_0(k, \epsilon - \epsilon_{q/2}) G_0(k + \tfrac{1}{2}q, \epsilon + \omega) \\ \times G_0(k - \tfrac{1}{2}q, \epsilon).\end{aligned} \tag{3.18}$$

It follows from Eqs. (3.17) and (2.7) that

$$\Pi(q, \omega) = -s_q \omega_q^0 I(q, \omega)/[1 - \tilde{I}(q, \omega)] \,. \tag{3.19}$$

To evaluate $\tilde{I}(q, \omega)$ we note again that the main contribution to the integral in Eq. (3.18) comes from $k = 0$, so that the vertex renormalization is due to small-momentum phonons. Taking $\omega_k^0 = v_s^0 k$, $\omega_k = v_s k$, and $(\epsilon_{k+q/2} - \epsilon_{q/2}) \simeq \pm k v_F$, and using Eq. (2.2), we can write, near $q = 2p_F$,

$$\begin{aligned}g_k^2 D(k, \epsilon - \epsilon_{q/2}) \simeq (2\pi^3 s_0/\beta m p_F) \\ \times \frac{(v_s^0 k)^2}{[(v_F k)^2 - (v_s k)^2]} \,,\end{aligned} \tag{3.20}$$

where s_0 is the coupling-strength parameter at $q = 0$. It follows that near $q = 2p_F$, $\tilde{I}$ has the form

$$\tilde{I}(q, \omega) \simeq [s_0 v_s^{0^2}/(v_F^2 - v_s^2)] I(q, \omega). \tag{3.21}$$

The function $\tilde{I}(q, \omega)$ has the same singularities as $I(q, \omega)$ and, hence, the function $\Pi(q, \omega)$ given by Eq. (3.19) has no divergences. If $v_s, v_s^0 \ll v_F$, then $\tilde{I}(q, \omega)$ contains a small coefficient $(v_s^0/v_F)^2$ and it, therefore, affects the phonon spectrum only in a close neighborhood of the singularity lines $\pm 2v_F q' = \omega$. It follows from Eqs. (3.1) and (3.21) that this neighborhood is defined by

$$|(2v_F q')^2 - \omega^2|/8\epsilon_F \lesssim \exp[-(4/s_0)(v_F/v_s^0)^2] \,. \tag{3.22}$$

Only the solution with $\omega \neq 0$, $\gamma = 0$ (Fig. 2) passes in the vicinity of these singularity lines. One can show from Eq. (3.9) that this solution satisfies

$$|(2v_F q')^2 - \omega^2|/8\epsilon_F > e^{-4/s_q} \,. \tag{3.23}$$

Assuming that s_q is of the same order of magnitude as s_0, we conclude that the solutions of Sec. IIIB do not come sufficiently close to the singularity lines to be affected significantly by $\tilde{I}(q, \omega)$. This is confirmed by a numerical calculation in-

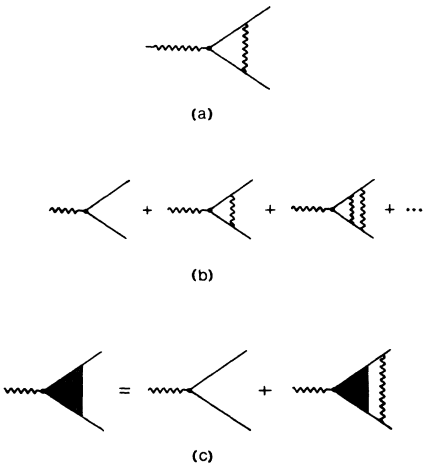

FIG. 3. Diagrammatic representation of (a) the lowest-order correction to Γ, (b) the ladder-diagram approximation for Γ, and (c) the Dyson equation for Γ in this approximation.

cluding the analytically continued function $I(q,\omega,\gamma)$. The calculation was performed with the exact function defined in Eq. (3.18) and not with the approximate expression (3.21). For $v_s^0/v_F = 0.01-0.1$ and $s = 0.25$, we find deviations of at most 5% from the solutions of Eqs. (3.9) and (3.10). At finite temperatures the effect of $\tilde{I}(q,\omega)$ is even less important, because then the singularity in $I(q,\omega)$ is smeared out and appears as $\ln(T/T_F)$. One should, however, keep in mind that other higher-order diagrams might affect the phonon spectrum more significantly than the ladder diagrams. Diagrams with intersecting phonon lines yield divergences due to $q = 2p_F$ phonons,[1] and "Parquet" diagrams must also be considered.[25]

IV. DEFORMED LATTICE

The occurrence of solutions with $\omega = \gamma = 0$ at a finite q indicates that the state with equidistant ions, on which the calculation was based, is not the ground state of the system and that a lower energy can be obtained with a distorted lattice. Let us assume a static deformation characterized by a single wave vector q. The deviation of the jth ion from its equilibrium position R_j in the regular lattice is given by

$$u_j = u_q(e^{iqR_j} + e^{-iqR_j}) \ . \tag{4.1}$$

Such a static deformation mixes the single-particle states with momenta $p, p\pm q$ and the new electron energies are eigenvalues of the matrix

$$\begin{pmatrix} \epsilon_{p+q} & \Delta_q & 0 \\ \Delta_q^* & \epsilon_p & \Delta_q^* \\ 0 & \Delta_q & \epsilon_{p-q} \end{pmatrix}, \tag{4.2}$$

where ϵ_p is the electron energy in the equidistant lattice, and

$$\Delta_q = u_q \langle p+q \,|\nabla U\,| p \rangle \tag{4.3}$$

or, $\Delta_q = u_q \nabla \langle p+q\,|U|p\rangle$, following Barisic.[5] ∇U being the gradient of the electron-ion potential. In addition to the change in the electronic energy, the deformation introduces an elastic energy density equal to (in the harmonic approximation)

$$E_D = NM\omega_q^0 u_q^2 \ , \tag{4.4}$$

where N is the density of ions and M is their mass. It is convenient to express this energy by means of Δ_q, which will serve as the variation parameter. Using Eqs. (4.3), (2.3), and (2.2), we find

$$E_D = (\beta m p_F/2\pi^3 s_q)\Delta_q^2 \tag{4.5}$$

The total energy density of the system is

$$\begin{aligned} E_T &= [2/(2\pi)^3]\int n_p \tilde{\epsilon}_p(\Delta_q) d^3p + E_D \\ &= (m\beta p_F/s_q\pi^3)[(s_q p_F/4m)\int n_p \tilde{\epsilon}_p(\Delta_q)\, dp + \tfrac{1}{2}\Delta_q^2] \ , \end{aligned} \tag{4.6}$$

where $\tilde{\epsilon}_p(\Delta_q)$ is that eigenvalue of (4.2) which satisfies $\tilde{\epsilon}_p(\Delta_q = 0) = \epsilon_p$. Let us now minimize the total energy by varying Δ_q. Since $\tilde{\epsilon}_p(\Delta_q)$ is a function of Δ_q^2, we find that

$$\left.\frac{\partial E_T}{\partial \Delta_q}\right|_{\Delta_q=0} = 0 \ , \tag{4.7}$$

so that the undeformed state always corresponds to an extremum of the energy. To find if it is a minimum, we have to consider the second derivative. One easily finds that

$$\left.\frac{\partial^2 \tilde{\epsilon}_p(\Delta_q)}{\partial \Delta_q^2}\right|_{\Delta_q=0} = \frac{2}{\epsilon_p - \epsilon_{p-q}} - \frac{2}{\epsilon_{p+q} - \epsilon_p} \ . \tag{4.8}$$

Therefore,

$$\left.\frac{\partial^2 E_T}{\partial \Delta_q^2}\right|_{\Delta_q=0} = \frac{m\beta p_F}{s_q\pi^3}\left[1 + \frac{s_q p_F}{4m}\int\left(\frac{2}{\epsilon_p - \epsilon_{p-q}} - \frac{2}{\epsilon_{p+q} - \epsilon_p}\right) n_p\, dp\right] = \frac{m\beta p_F}{s_q\pi^3}\left[1 - 2s_q\ \mathrm{Re} I(q, \omega = 0)\right] . \tag{4.9}$$

The last equality is based on Eqs. (2.6) and (2.7). The undeformed state is stable and corresponds to a minimum of energy if the expression in the brackets is positive for all q. This is exactly the condition for the nonexistence of phonon excitations with $\omega = 0$. If this condition is not satisfied, as it always happens for $T = 0$ at $q = 2p_F$, one has to look for another solution of the equation $\partial E_T/\partial \Delta_q = 0$.

Let us now assume a deformation characterized by the wave vector $q = 2p_F$. In this case it is sufficient to consider the 2×2 matrix

$$\begin{pmatrix} \epsilon_p & \Delta \\ \Delta^* & \epsilon_{p-2p_F} \end{pmatrix} , \tag{4.10}$$

where we have dropped the index $2p_F$ of Δ. The eigenvalues of this matrix are

$$\epsilon_p^{\pm}(\Delta) = \tfrac{1}{2}(\epsilon_{p-2p_F} + \epsilon_p) \pm \tfrac{1}{2}[(\epsilon_{p-2p_F} - \epsilon_p)^2 + 4\Delta^2]^{1/2} \ . \tag{4.11}$$

A gap of 2Δ appears in the electron spectrum at $p = p_F$. The condition $\partial E_T/\partial \Delta_q = 0$ yields the equation

$$\frac{s p_F}{4m}\int \frac{2n_p dp}{2\tilde{\epsilon}_p(\Delta) - (\epsilon_p + \epsilon_{p-2p_F})} + 1 = 0 \ , \tag{4.12}$$

where $s = s_{2p_F}$ and $\tilde{\epsilon}_p(\Delta)$ is the solution with the minus sign [Eq. (4.11)]. Assuming again a free-particle dispersion $\epsilon_p = p^2/2m$, we find for $T = 0$

that the energy attains a minimum when Δ satisfies the equation

$$1+\tfrac{1}{2}s\,\ln(p_F^2/m\Delta)[(1+m^2\Delta^2/p_F^4)^{1/2}-1]\}=0\,. \quad (4.13)$$

For $\Delta \ll 2\epsilon_F (s<\tfrac{1}{2})$, the solution of this equation is approximated by

$$\Delta = 4\epsilon_F e^{-\frac{2}{s}}, \quad (4.14)$$

which is essentially the result of Fröhlich.[10]

We concluded in Sec. III that the lattice is unstable for any q for which s_q exceeds $s_c(q)$. We expect that the deformation with $q=2p_F$ will stabilize the lattice against any other deformation. To see this explicitly, let us calculate the phonon dispersion of the distorted lattice in the neighborhood of $q=2p_F$. Since this is affected only by electrons near the Fermi surface, we may approximate the electron energies by

$$\epsilon_p = \begin{cases} p^2/2m-\Delta\,, & |p|<p_F \\ p^2/2m+\Delta\,, & |p|>p_F\,. \end{cases} \quad (4.15)$$

This is a somewhat crude approximation, since $\partial\epsilon_p/\partial p$ should vanish as $p\to p_F$. Using this dispersion in Eq. (2.6), we obtain an account of Eq. (2.7),

$$\mathrm{Re}I(q,\omega)=\frac{p_F}{4q}\ln\left|\left(\frac{(p_F+q/2+2m\Delta/q)^2-(m\omega/q)^2}{[p_F-q/2+(2m\Delta/q)\mathrm{sgn}(2p_F-q)]^2-(m\omega/q)^2}\right)\right|, \quad (4.16)$$

$$\mathrm{Im}I(q,\omega)=(\pi p_F/4q)[\theta(|\tfrac{1}{2}q+m\omega/q-2m\Delta/q|-p_F)-\theta(p_F-|\tfrac{1}{2}q-m\omega/q+2m\Delta/q|)]\,. \quad (4.17)$$

These expressions are very similar to Eqs. (3.1) and (3.2), except that the region of electron-hole excitations (namely, the region in which $\mathrm{Im}I(q,\omega)\neq 0$) around $q=2p_F$ is shifted upwards by Δ and so are the singularity lines $\omega=\pm 2v_F|q'|$. Inserting Eq. (4.16) into Eq. (2.9) and assuming $\Delta\ll\epsilon_F$, we find that $\omega=0$ is a solution at $q=2p_F$ if Δ satisfies the equation

$$1-(s/2)\ln(4\epsilon_F/\Delta)=0. \quad (4.18)$$

For this Δ, $\omega=0$ is not a solution at any other q. But Eq. (4.18) is equivalent to Eq. (4.14), meaning that the gap which minimizes the energy yields a real zero energy phonon "excitation" at $q=2p_F$, corresponding to the static distortion, and stabilizes the lattice at all other momenta.

We have solved Eq. (2.9) with $I(q,\omega)$ given by Eqs. (4.16) and (4.17), and Δ given by Eq. (4.14), in the complex ω plane. The solution is plotted in Fig. 4 for $s=0.25$ and $\alpha=0.01$. We find again two phonon branches. The lower branch is undamped and it has a cusp at $2p_F$. The higher branch is damped and it exists only in the region in which $\mathrm{Im}I(q,\omega)\neq 0$. This branch disappears when $\Delta>\omega_0$, as is the case, for $s=0.325$ (Fig. 4). The spectral density function $B(q,\omega)$ for the solution represented in Fig. 4 is plotted, for several values of the momentum around $2p_F$, in Fig. 5. This function consists of a δ-function peak corresponding to the undamped branch and of a continuous part representing the phonon spectral weight in the region of electron-hole excitations. The function $B(q,\omega)$ satisfies the sum rule

$$\int_0^\infty (\omega/\omega_0)B(q,\omega)\,d\omega=1. \quad (4.19)$$

The height of the arrows representing the δ function in Fig. 5 is equal to the contribution of the undamped branch to this sum rule, and it approaches unity when $|q-2p_F|>\omega_0/v_F$ ($x\gtrsim 0.002$, in Fig. 5). For such values of q there is only negligible phonon spectral density in the region of electron-hole excitations.

V. PHONON DISPERSION SAWADA MODEL

To complete the discussion of the phonon dispersion at $T=0$, we shall now treat the problem within the framework of the Sawada model.[12]

Let us first reformulate the Hamiltonian in Eq. (2.1) so that the gap in the single-electron spectrum resulting from the static deformation will appear explicitly. This can be done systematically by treating the phonon operators a_{2p_F}, $a^\dagger_{2p_F}$ as c-numbers in a manner similar to the Bogoliubov method in liquid helium. The terms involving these operators may then be incorporated in the electron kinetic energy, modifying the electron energies and the electron creation and destruction operators. We shall not dwell upon the details of this step and simply write the Hamiltonian

$$H=\sum_p \tilde{\epsilon}_p \tilde{c}^\dagger_p \tilde{c}_p+\sum_{q\neq 2p_F}\omega_q^0 a_q^\dagger a_q + \sum_{p,q\neq 2p_F} g_q(a_q+a_{-q}^\dagger)\tilde{c}^\dagger_{p+q}\tilde{c}_p\,, \quad (5.1)$$

where $\tilde{\epsilon}_p$ are the energies of electron states in the distorted lattice [Eq. (4.11)], and $\tilde{c}_p$, $\tilde{c}^\dagger_p$ are their destruction and creation operators.

Let us now apply the Sawada method to this Hamiltonian. This method treats the particle-hole ex-

citation as a single entity and takes into account only terms which involve the creation, destruction, and scattering of such excitations. The particle-hole destruction operators are

$$d_q(p)=\tilde{c}_p^\dagger \tilde{c}_{p+q} . \tag{5.2}$$

Here, and in what follows, $|p+q|>p_F$, $|p|<p_F$. The basic assumption of the Sawada method is that these operators satisfy the Bose commutation relations

$$[d_q(p),\ d_{q'}(p')]=[d_q^\dagger(p),\ d_{q'}^\dagger(p')]=0 , \tag{5.3}$$

$$[d_q(p),\ d_{q'}^\dagger(p')]=\delta_{qq'}\delta_{pp'} . \tag{5.4}$$

To estimate the validity of this assumption we evaluate the expectation values of these commutation relations in the ground state of the Hamiltonian (5.1):

$$\langle 0|[d_q(p),\ d_{q'}^\dagger(p')]|0\rangle=\delta_{pp'}\delta_{qq'}[\tilde{n}_p-\tilde{n}_{p+q}], \tag{5.5}$$

where $\tilde{n}_p$ is the occupation number in the interacting ground state. The expectation values of the other commutation relations vanish exactly. It is clear from Eq. (5.5) that the validity of the Sawada assumption depends on how close is the interacting ground state to a filled Fermi sea. Putting it differently, it is assumed that

$$\tilde{c}_{p+q}|0>\simeq 0, \qquad c_p^\dagger|0>\simeq 0. \tag{5.6}$$

The Sawada model Hamiltonian is in our case

$$H_s=\sum_p \tilde{\epsilon}_p \tilde{c}_p^\dagger \tilde{c}_p+\sum_{q\neq 2p_F}\omega_q^0 a_q^\dagger a_q+ \\ +\sum_{p,\,q\neq 2p_F} g_q(a_q+a_{-q}^\dagger)[d_q^\dagger(p)+d_{-q}(-p)] . \tag{5.7}$$

The excitation energies of this Hamiltonian may be found from the equation

$$[H_s,\eta_q^\dagger]=\omega_q\eta_q^\dagger . \tag{5.8}$$

The operators $n_q^\dagger$, which generate the excited states, are assumed to be of the form

$$n_q^\dagger=\alpha_q(a_q^\dagger+a_{-q})+\beta_q(a_q^\dagger-a_{-q})+\sum_p[A_q(p)d_q^\dagger(p) \\ +B_q(p)d_{-q}(-p)] \tag{5.9}$$

Comparing the two sides of Eq. (5.8), we obtain equations for the coefficients α_q, β_q, $A_q(p)$, $B_q(p)$:

$$\begin{aligned}
&\alpha_q\omega_q=\beta_q\omega_q^0+g_q\sum_p[A_q(p)-B_q(p)] ,\\
&\beta_q\omega_q=\alpha_q\omega_q^0 ,\\
&A_q(p)\omega_q=2\beta_q g_q+A_q(p)(\epsilon_{p+q}-\epsilon_p) ,\\
&B_q(p)\omega_q=2\beta_q g_q-B_q(p)(\epsilon_{p+q}-\epsilon_p) .
\end{aligned} \tag{5.10}$$

Multiplying the first two of these equations by each other and inserting the expressions for $A_q(p)$, $B_q(p)$ derived from the last two, we obtain an equation for the excitation energy ω_q,

$$\omega_q^2=\omega_q^{0^2}+2\omega_q^0 F(q,\omega_q) , \tag{5.11}$$

where

$$F(q,\omega_q)=g_q^2\sum_p\left(\frac{1}{\omega_q-\epsilon_{p+q}+\epsilon_p}-\frac{1}{\omega_q+\epsilon_{p+q}-\epsilon_p}\right) . \tag{5.12}$$

Note that except for a factor of 2 (coming from the two spin states which we have ignored here),

$$F(q,\omega)=\mathrm{Re}\,\Pi_0(q,\omega). \tag{5.13}$$

An additional equation is needed to fix the coefficients in $\eta_q^\dagger$, and this comes from the normalization condition

$$[\eta_q,\eta_{q'}^\dagger]=\left(4\alpha_q\beta_q+\sum_p[A_q^2(p)-B_q^2(p)]\right)\delta_{qq'}=\delta_{qq'}. \tag{5.14}$$

The commutation relations of two η_q-s or two $\eta_q^\dagger-s$ vanish because $A_q(p)=A_{-q}(-p)$, $B_q(p)=B_{-q}(-p)$. From Eq. (5.14) we obtain, on account of Eqs. (5.10) and (5.12),

$$\beta_q^2=\frac{1}{4}\left(\frac{\omega_q}{\omega_q^0}-\frac{\partial}{\partial\omega_q}F(q,\omega_q)\right)^{-1}. \tag{5.15}$$

Let us now derive the phonon spectral density function $B(q,\omega)$. We start from the general definition[26]

$$B(q,\omega)=\sum_m[|\langle m|\phi_q^\dagger|0\rangle|^2\delta(\omega-\omega_m) \\ -|\langle m|\phi_q|0\rangle|^2\delta(\omega+\omega_m)] , \tag{5.16}$$

where $\phi_q=a_q+a_{-q}^\dagger$, and m is an excited state with energy ω_m. Putting $n_q^\dagger|0\rangle=|m\rangle$, and using $n_q|0\rangle=0$ and the commutation relations

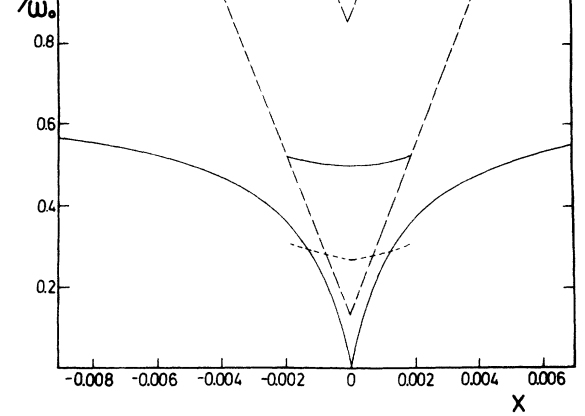

FIG. 4. Typical phonon dispersion of the deformed lattice at $T=0$, for $s=0.25$ and $\alpha=0.01$. The broken curve is the imaginary part of the damped branch, which exists only between the singularity lines (broken lines). When $s=0.325$, these lines are too high for the damped branch to occur. The cusp in the broken curve at $x=0$ is a spurious result, caused by the crudeness of approximation (4.15).

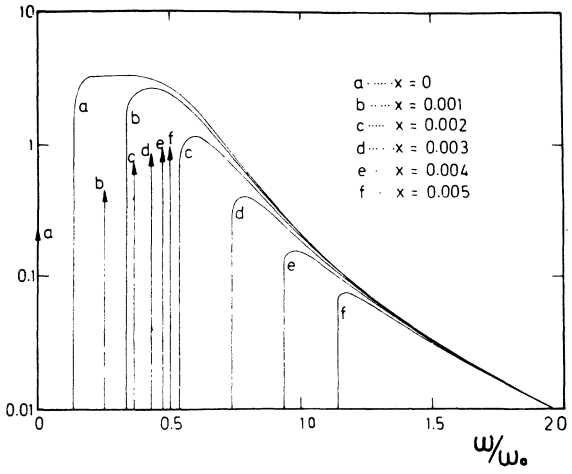

FIG. 5. Spectral density $B(q, \omega)$ in the distorted lattice at $T=0$ for $\alpha=0.01$, $s=0.25$ and for various values of q around $2p_F$, measured in units of $x=(q-2p_F)/2p_F$. The vertical arrows correspond to the undamped branch and their height is the contribution of this branch to the sum rule in Eq. (4.19).

$$[\phi_q, \eta_{q'}] = -2\beta_q \delta_{q,-q'} ,$$
$$[\phi_q^\dagger, \eta_{q'}] = -2\beta_q \delta_{q,q'} , \tag{5.17}$$

we obtain

$$B(q, \omega) = 4\beta_q^2[\delta(\omega-\omega_q) - \delta(\omega+\omega_q)] . \tag{5.18}$$

Equation (5.8) provides only the undamped excitations, and hence, Eq. (5.11) describes the lower branch of Sec. IV starting from the definition of $B(q, \omega)$ given in Eq. (3.13), we find that in this case (for $\omega > 0$)

$$B(q, \omega) = 2\omega_q^0 \delta[\omega^2 - \omega_q^{0^2} - 2\omega_q^0 \,\mathrm{Re}\Pi_0(q, \omega)]$$
$$= \delta(\omega-\omega_q) \Big/ \left| \frac{\omega}{\omega_q^0} - \frac{\partial}{\partial\omega} \mathrm{Re}\Pi_0(q, \omega \right|_{\omega=\omega_q}^{-1} \tag{5.19}$$

This is consistent with Eq. (5.18), in view of Eqs. (5.15) and (5.13).

We have reproduced the results of RPA for the energies and spectral densities of the undamped branch of the phonon spectrum, but in addition to that, the Sawada model provides us with a description of the structure of the excitations. The sum of the coefficients $A_q(p)$, $B_q(p)$ measures the admixture of the electron-hole states in the phonon excitation. One can easily show that this admixture increases with $|\omega_q - \omega_q^0|$ and attains its maximum near $q = 2p_F$.

In conclusion, let us discuss the validity of the underlying assumptions of the Sawada method, namely, Eq. (5.4) or (5.6). Since $\eta_q|0\rangle = 0$, the condition $\tilde{c}_p^\dagger|0\rangle \simeq 0$ will be satisfied if $[\eta_q, \tilde{c}_p^\dagger] \simeq 0$.

It follows from Eq. (5.9) that

$$[\eta_q, \tilde{c}_p^\dagger] = A_q(p)\tilde{c}_{p+q}^\dagger . \tag{5.20}$$

Let us make a rough estimate of $A_q(p)$. Equations (5.10) and (5.12) imply that

$$F(q, \omega_q) = \frac{g_q}{2\beta_q} \sum_p [A_q(p) - B_q(p)] . \tag{5.21}$$

The electron-energy differences $\epsilon_{p+q} - \epsilon_p$ have a lower bound of 2Δ. We mentioned that the coefficients $A_q(p)$ increase as ω_q departs from ω_q^0. Therefore, if we can justify the Bose commutation relations for $\omega_q < 2\Delta$, they will certainly hold for larger values of ω_q. For such ω_q the $A_q(p)$ coefficients are negative and so is $F(q, \omega)$. It follows from Eq. (5.12) that

$$|F(q, \omega)| \lesssim \tfrac{1}{2}\omega_q^0 , \tag{5.22}$$

and therefore

$$\frac{\beta_q \omega_q^0}{2g_q} \gtrsim \sum_p [\,|A_q(p)| + |B_q(p)|\,] . \tag{5.23}$$

The terms in the sum do not depend strongly on p, so that

$$|A_q(p)| \simeq |B_q(p)| < \frac{1}{N}\frac{\beta_q\omega_q^0}{4g_q}$$
$$= \frac{1}{N}\frac{\omega_q^0}{4g_q}\left(\frac{\omega_q^0}{\omega_q}\right)^{1/2}\left(\frac{B(q, \omega_q)\omega_q}{\omega_q^0}\right)^{1/2} . \tag{5.24}$$

The last factor is bounded by unity due to the sum rule [Eq. (4.19)]. The right-hand side diverges for $\omega_q = 0$, which happens at $q = 2p_F$, but the term corresponding to this momentum has been excluded from the Hamiltonian. When $(\omega_q/\omega_q^0) \gg 1/N$, the coefficients $A_q(p)$ are very small and the Sawada model is valid.

VI. PHONON DISPERSION AT $T \neq 0$

In the present section we extend the calculation of the phonon dispersion to finite temperatures and derive the critical temperature T_p of the Peierls-Fröhlich instability. The only difference from the $T=0$ case is that now in Eq. (2.8),

$$n_p = \left\{\exp\left[\frac{1}{kT}\left(\frac{p^2}{2m} - \mu\right)\right] + 1\right\}^{-1} . \tag{6.1}$$

We shall restrict ourselves to $T \ll T_F$ (the Fermi temperature) which is justified as long as $T_p \ll T_F$. For such low temperatures we may put $\mu = p_F^2/2m$, independent of T. The Fermi-Dirac function may be approximated in this region by an inclined step function with the correct slope at the Fermi energy:

$$n_p=\begin{cases}1, & 0\le|p|\le p_F(1-\tau)\\ \frac{1}{2\tau}\left(1+\tau-\frac{|p|}{p_F}\right), & p_F(1-\tau)\le|p|\le p_F(1+\tau)\\ 0, & p_F(1+\tau)\le|p|\end{cases} \tag{6.2}$$

where $\tau=2mkT/p_F^2=T/T_F$. With this approximation for n_p one can calculate explicitly the function $I(q,\omega,\tau)$ defined in Eq. (2.8). Being interested only in the vicinity of $q=2p_F$, it is now convenient to denote $x=(q-2p_F)/2p_F$, $y=\omega/4\epsilon_F$. One obtains for $x,y\ll 1$,

$$\begin{aligned}\mathrm{Re}I(x,y,\tau)=-\frac{1}{16\tau}\{&(x+y+\tau)\ln|x+y+\tau|\\&+(x-y+\tau)\ln|x-y+\tau|\\&-(x+y-\tau)\ln|x+y-\tau|\\&-(x-y-\tau)\ln|x-y-\tau|\}\\&+\tfrac{1}{8}(2+\ln 4),\end{aligned} \tag{6.3}$$

$$\mathrm{Im}I(x,y,\tau)=-\frac{\pi}{8}\left(\frac{1}{\exp[(2/\tau)(x+y)]+1}-\frac{1}{\exp[(2/\tau)(x-y)]+1}\right). \tag{6.4}$$

The imaginary part is evaluated with the exact form of n_p. The singularity in ReI along the lines $y=\pm x$, found for $\tau=0$, is smeared out at $\tau\neq 0$. Instead, we now find four lines $y=\pm x\pm\tau$, on which ReI has a logarithmic divergence in the derivative. This, however, is a result of the two discontinuities in our trapezoidal approximation for n_p and has no physical significance.

The critical temperature T_p is the temperature for which $\omega=0$, $\gamma=0$ is a solution of Eq. (2.9) at $q=2p_F$, and is therefore determined by the equation

$$1=2s\ \mathrm{Re}I(0,0,T_p/T_F). \tag{6.5}$$

With Eq. (6.3), one gets

$$T_p=2T_F e^{1-2/s}. \tag{6.6}$$

A similar result was obtained by Kuper.[27] Comparing this with the gap in the electron spectrum, which minimizes the energy at $T=0$ [Eq. (4.14)] we find $\Delta=1.47T_p$. Equation (6.6) is correct only when $T_p\ll T_F$, namely, for $s\lesssim 0.5$.

When the coupling is stronger it is possible to get an instability at $q\neq 2p_F$. To see how this may happen let us consider the critical coupling parameter $s_c(q,\tau)$, defined by the equation

$$1=2s_c(q,\tau)I(q,0,\tau), \tag{6.7}$$

which is the finite-temperature form of Eq. (3.12). This parameter is plotted for several values of τ in Fig. 6. The lattice is unstable for any q, for which $s_q\ge s_c(q,\tau)$. The actual distortion of the lattice will occur at that q, for which $s_q=s_c(q,\tau_{\max})$.

It is clear from the figure, that as long as s_{2p_F} is not too large ($s\lesssim 0.5$), any reasonable dependence of s_q on q will lead to an instability at $q=2p_F$. When $s>0.5$, then T_p is large and the corresponding curve of the critical parameter has a shallow minimum, so that it is sufficient that s_q at some $q\neq 2p_F$ will exceed slightly s_{2p_F} in order to get an instability for this q at a temperature higher than T_p. To explain the martensitic transitions in β-tungstens, Barisic[5] treats a similar model with a strong coupling ($s\simeq 1$). In this case $T_p\lesssim T_F$ and the critical curve $s_c(q,T_p)$ is very flat, so that a modest variation of s_q may cause an instability at $q=0$ before $q=2p_F$ (if $s_0\gtrsim 1$ and $s_{2p_F}\lesssim 0.7$). Empirically it is found that the lattice prefers to distort with wave vectors $q=0$ or $q=\pi/a$. An appropriate variation of s_q with q can account for this observation even if $2p_F\neq 0$, π/a, or $2\pi/a$.

Let us now calculate the phonon dispersion for $T\gtrsim T_p$. To this end we continue analytically the function $I(q,\omega,\tau)$ to the complex equation

$$(\omega+i\gamma)^2=\omega_0^2[1-2sI(q,\omega,\gamma,\tau)]. \tag{6.8}$$

We assume again that ω_q^0 and s_q do not depend on q. The solution of this equation for $s=0.25$ and $\alpha=\omega_0/2\epsilon_F=0.1$ is plotted in Figs. 7 and 8. In Fig. 7, $\tau=0.0018$, which for the given value of s corresponds to $T=T_p$. The general behavior is similar to the $T=0$ case, but now one gets a solution with $\omega=0$, $\gamma=0$ at $q=2p_F$, and except at this point both branches have an imaginary part. Figure 8 corresponds to a considerably higher temperature ($\tau=0.02$) and shows a drastic change in the nature of the solutions. The lower branch exists only in a narrow neighborhood of $2p_F$ and is strongly damped there, and now it is the higher branch which joins smoothly with the unperturbed dispersion curve $\omega(q)=\omega_0$ outside the region of $q\simeq 2p_F$.

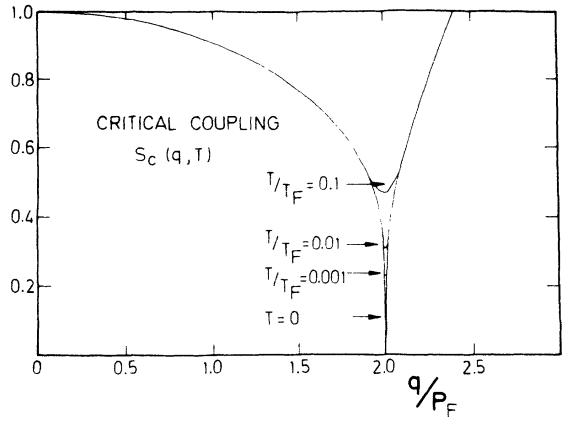

FIG. 6. Critical coupling curves $s_c(q, T)$ for several values of $\tau=T/T_F$.

Let us now describe the phonon excitation spectrum by means of the spectral density function $B(q, \omega)$. This function (actually multiplied by ω_0 to make it dimensionless) is plotted for various combinations of parameters in Figs. 9–11. We find that two distinct excitation branches exist at $q = 2p_F$ and its sufficiently close neighborhood as long as $T < T_{ph}$ ($T_{ph} = \omega_0$) which is the same as $\tau/2\alpha < 1$. For $T = T_{ph}$ (the $\tau = 0.02$ frame in Fig. 10) one can hardly resolve the two peaks, and for $T > T_{ph}$ only one peak appears. This is reminiscent of the condition $\Delta_p \leq \omega_0$, found in Sec. V, for the existence of two branches at $T = 0$ in the deformed lattice. As one moves away from the point $x = 0$ ($q = 2p_F$), the spread of the spectral density distribution decreases until only a single narrow peak appears for $x \gtrsim \omega_0/4\epsilon_F = \frac{1}{2}\alpha$ (see Fig. 9). Exactly as in the $T = 0$ case, the parameter α determines the width of the region around $q = 2p_F$, in which the electron-phonon interaction is most effective. The sum rule in Eq. (4.19) is independent of T and we used it to check our solutions. We found that our spectral-weight functions satisfy the sum rule extremely well for $T \leq T_p$ at all values of q.

Two excitation peaks were observed by Shirane and Axe[14] in neutron-scattering experiments on Nb_3Sn at $q = 0.02\pi/a$. The two peaks occur at about $\omega = 0$ and $\omega = 0.3$ meV and both have a width of $\omega = 0.1$ meV. The lower peak was observed at $T = 46\,^\circ$K and $T = 60\,^\circ$K, and the unperturbed frequency was found from high-temperature measurements to be $\omega_0 \simeq 0.6$ meV. Therefore, in this case $T \gg T_{ph}$, and if our idealized model were applicable here, only one branch should exist (provided that the given value of q corresponds to $2p_F$ of a very narrow band). Barisic *et al.*[13] have calculated the same spectral-density functions within the tight-binding approximation for the case of $\alpha = 0.1$ and reached a similar conclusion. The failure to explain the observation of Shirane and Axe within the framework of our simple model will be further discussed in Sec. VIII.

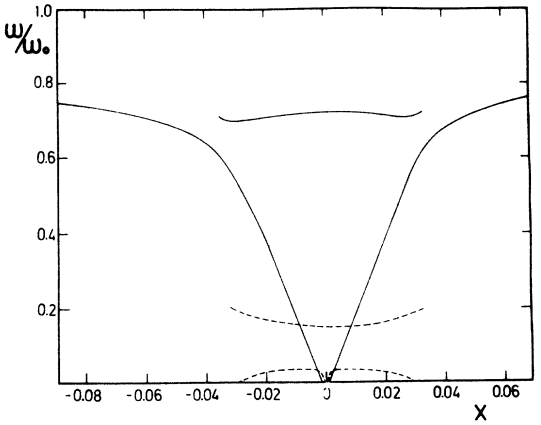

FIG. 7. Typical phonon dispersion near $q = 2p_F$, at $\tau = T/T_F = 0.0018$ ($T = T_p$), for $\alpha = 0.1$ and $s = 0.25$. The broken curves are the negative imaginary parts of the two branches. The higher broken curve corresponds to the higher excitation branch.

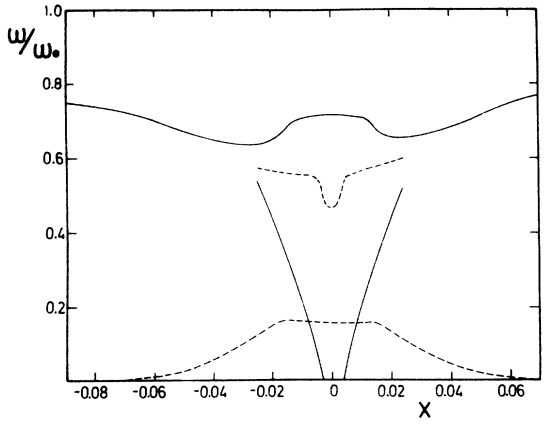

FIG. 8. Typical phonon dispersion at $T/T_F = 0.02$. The other parameters are the same as in Fig. 7. This time the higher broken curve corresponds to the lower excitation branch.

VII. CRITICAL VIBRATIONS

In this section we show that the mean-square deviation of the ions from their equilibrium position diverges as T approaches T_p, and find the critical-temperature region in which this divergence would prohibit the use of a linear electron-phonon interaction.

The deviation of the jth ion from equilibrium is given by

$$u_j = \sum_q \left(\frac{1}{2NM\omega_q^0}\right)^{1/2} \phi_q e^{iqR_j} . \tag{7.1}$$

The thermal average of u_j^2 is

$$\langle u_j^2 \rangle = \sum_q \frac{1}{2NM\omega_q^0} e^{\beta\Omega} \sum_m e^{-\beta\omega_m} \langle m | \phi_q \phi_q^\dagger | m \rangle , \tag{7.2}$$

where $e^{\beta\Omega} = \sum_m e^{-\beta\omega_m}$ ($\beta = 1/kT$). This average may be expressed by means of the spectral-density function $B(q, \omega)$, using the finite-temperature extension of Eq. (5.16)[28]

$$B(q, \omega) = e^{\beta\Omega} \sum_{m,n} e^{-\beta\omega_m}(1 - e^{-\beta\omega}) \times |\langle n | \phi_q^\dagger | m \rangle|^2 \delta(\omega + \omega_m - \omega_n). \tag{7.3}$$

From Eqs. (7.2) and (7.3), we get

$$\langle u_j^2 \rangle = \frac{1}{2NM} \sum_q \frac{1}{\omega_q^0} \int_{-\infty}^{\infty} \frac{B(q, \omega)\, d\omega}{1 - e^{-\beta\omega}} . \tag{7.4}$$

This expression diverges in the one-dimensional case due to the contribution of the low-momentum

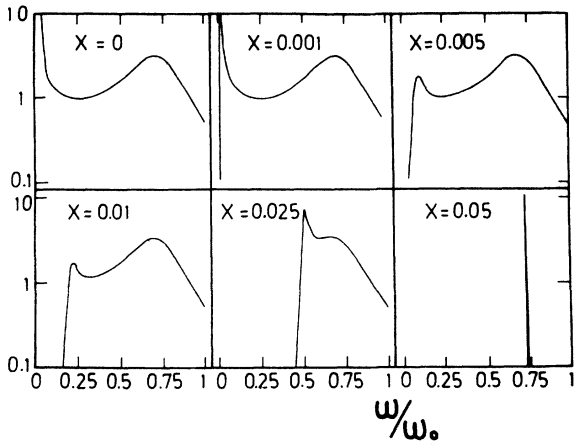

FIG. 9. The function $\omega_0 B(q, \omega)$ for $\alpha = 0.1$, $s = 0.25$, $T/T_F = 0.0018$ $(T = T_p)$, and for various values of $x = (q - 2p_F)/2p_F$.

phonons, which is usually quoted as a proof for the nonexistence of one-dimensional crystals. Having discussed linear-chain crystals throughout this paper, we have implicitly ignored this divergence, assuming that in practice it is washed out by the weak coupling between different chains. In addition to this, there is also a divergent contribution to $\langle u_j^2 \rangle$ from the neighborhood of $q = 2p_F$ when $T \to T_p$. The function $B(q, \omega)$ diverges there as $\omega \to 0$ and, therefore, the main contribution to the ω integral in Eq. (7.4) comes from small ω. Thus, we have

$$\int_{-\infty}^{\infty} \frac{B(q,\omega)\, d\omega}{1 - e^{-\beta\omega}} \simeq \frac{2}{\beta} \int_0^{\infty} \frac{B(q,\omega)\, d\omega}{\omega} . \tag{7.5}$$

The integral on the right-hand side is the spectral representation of $D(q, \omega)$ at $\omega = 0$ and therefore, using Eqs. (2.4) and (2.7),

$$\int_0^{\infty} B(q,\omega)\, d\omega/\omega = 1/\omega_0[1 - 2sI(q, 0, \tau)] , \tag{7.6}$$

where, again, $\tau = T/T_F$ and ω_0, s are the values of these parameters at $q = 2p_F$. We next replace the sum in Eq. (7.4) by an integral and transform the integration variable to $x = (q - 2p_F)/2p_F$. Being interested in the neighborhood of $x = 0$, we expand $I(x, 0, \tau)$, given by Eq. (6.3), for small x, and obtain

$$\langle u_j^2 \rangle \simeq \frac{2k_B T}{sM\omega_0^2} \int \frac{dx}{2\ln(\tau/\tau_p) + (x/\tau)^2} \tag{7.7}$$

where $\tau_p = T_p/T_F$ is determined by (6.6). Extending the integration over x from $-\infty$ to $+\infty$, we get, as long as s is not too small $(\tau^2 \ln(T/T_p) \ll 1)$

$$\langle u_j^2 \rangle \frac{2\pi(k_B T)^2}{sE_F M\omega_0^2} \frac{1}{[2\ln(T/T_p)]^{1/2}} \tag{7.8}$$

comparing this to the zero-point fluctuations in the absence of electron-phonon coupling, $\langle u_j^2(0) \rangle = \hbar/M\omega_0$, we finally get

$$\frac{\langle u_j^2 \rangle}{\langle u_j^2(0) \rangle} = 2\pi \frac{k_B T}{E_F} \frac{k_B T}{\hbar\omega_0} \frac{1}{s[2\ln(T/T_p)]^{1/2}} . \tag{7.9}$$

If we define the critical region as the region where the thermal fluctuations equal the zero-point vibrations (admittedly, a somewhat arbitrary definition, but probably adequate for order-of-magnitude estimates), then we get for $k_B T_p \approx \hbar\omega_0 \approx 10^{-2} E_F$, $s \approx 0.3$ that the width of the critical region is $(T - T_p)/T_p \approx 10^{-1}$, very roughly.

In this context, we may mention some experiments that may bear relevance to the possible existence of a large critical region in the quasi-one-dimensional A-15 compounds. Shier and Taylor[29] claim, from Mössbauer effect data, that there are strong fluctuations over a wide temperature region in Nb_3Sn; Testardi[30] observed strong frequency doubling of sound waves in V_3Si; Fradin, Knapp, and Kimball[31] found anomalies in the specific heat of V_3Ga, V_3Si that suggest a highly nonlinear behavior around 100 °K; this in addition to older experiments on these materials[1,32] that also indicate a highly nonlinear behavior.

VII. DISCUSSION

We have studied in this work the properties of the phonon-excitation spectrum in one-dimensional systems and the nature of the instability proposed by Peierls and Fröhlich. Attempting to relate our results to observations on real quasi-one-dimensional systems one should bear in mind that we made several far-reaching approximations: (a) We considered a strictly one-dimensional system, namely, a single linear chain, rather than a family of weakly coupled linear chains as in the organic conductors, or a network of three perpendicular interpenetrating linear chains as in the β-tungstens; (b) we considered only one electronic band with a free-electron dispersion $\epsilon_p = p^2/2m^*$, while real

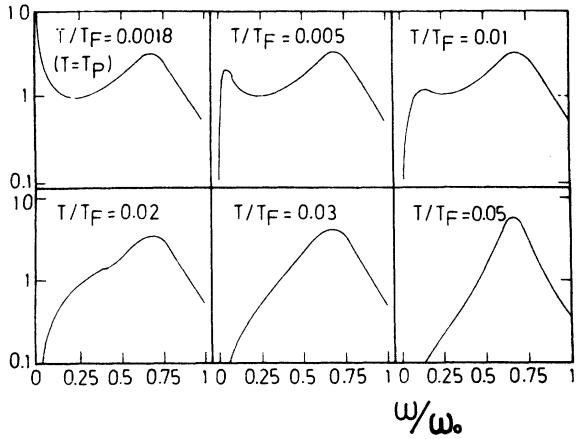

FIG. 10. Function $\omega_0 B(q, \omega)$ for $\alpha = 0.1$, $s = 0.25$, $q = 2p_F$, and various values of T/T_F.

materials have a more complicated band structure; (c) we have neglected the Coulomb interaction between the electrons.

With a simple model based on these assumptions, we found that under certain conditions two branches exist in the excitation spectrum near $2p_F$. These two branches are mixtures of an electron-hole ("charge-oscillation") excitation and a phonon. The width of the higher branch at temperatures close to T_p is of the order of $k_B T_p$ (see Figs. 9–11). Thus, the two branches can be resolved only if the bare-phonon frequency exceeds considerably $k_B T_p$. This would be the case for optical phonons, but not for acoustic phonons with a small wave vector, such as those investigated by Shirane and Axe.[14]

Each of the assumptions mentioned above simplify considerably the actual situation in a β-tungsten crystal and, thus may be responsible for the failure of our model to explain the results of Ref. 14. Although the low momentum $q \simeq 0.02\pi/a$, at which the phonon softening and the central peak are observed, may correspond to $2p_F$ of a very narrow one-dimensional subband, it is also possible that this value of q is completely unrelated to $2p_F$. Even if the electron dispersion is one-dimensional, the phonon spectrum may be far from the one-dimensional character $\omega(q) = \omega(q_z)$ considered here. The assumption $\omega(q) = \omega(q_z)$ is certainly wrong for accoustical phonons; but it may be a reasonable assumption for optical phonons, which may be approximated by an Einstein spectrum. A simple model which incorporates some of the properties of a β-tungsten structure is a network of two interpenetrating orthogonal families of chains.[33] It is assumed that the electrons are constrained to move along the chains and that there are force constants between two neighboring ions belonging to the same chain and to two orthogonal chains. There are four phonon branches LA, LO, TA, TO in this planar network. Depending on the values of the force constants and of p_F, one finds that the instability may occur at $q = 0$, π/a or $2\pi/a$ rather than at $q = 2p_F$, and it may be associated with the LA or the LO branch. The details of this planar network model are presently under investigation. Actually, there may also be electron-transfer between the chains, which complicates things even further, because then the effective coupling may depend strongly on the direction of q. It may, for example, reach a maximum for a TA phonon at 45° with respect to the linear chains (in this planar network model), or for a [110] phonon polarized in the $[1\bar{1}0]$ direction in a three-dimensional system such as the β-tungsten structure.

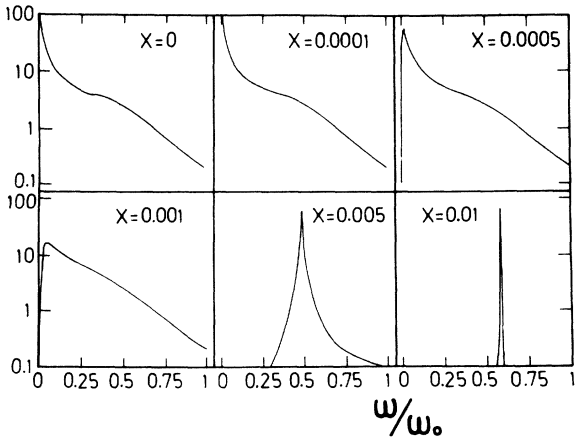

FIG. 11. Same as Fig. 9, except for $\alpha = 0.01$.

In a system with several electronic bands, electrons may shift from one band to another as the lattice is distorted. Such a process may be nonadiabatic. Consider, for example, a single chain in the z direction with two d bands: $\sigma(z^2 - \frac{1}{3}r^2)$ and $\delta_2(xy)$. As the lattice is compressed, the σ band may lower its energy more than δ_2 band (due to a larger overlap and/or a larger effect on the crystal-field integrals). A longitudinal distortion cannot provide the angular momentum required to transfer an electron from the $\delta_2(m_l = \pm 2)$ to the $\sigma(m_l = 0)$ band. Thus, the angular momentum must come from some other source (for example, electron-electron collisions), and the band repopulation may be a relaxation process, which is not included in the present formalism.

One should keep in mind that the planar Fermi surface extending across the whole Brillouin zone is an idealization. In real β-tungsten one has to deal with a considerably smaller planar section of the Fermi surface, and thus with electron states that cannot be localized on individual chains. This feature can be accounted for, to some extent, by a smaller value of the parameter β [Eq. (2.2)] leading to a smaller value of s for a given coupling strength g.

Finally, let us discuss one effect of the Coulomb interaction between the electrons, which may be relevant for the explanation of the two peaks observed in Ref. 14. It is known that the Coulomb interaction gives rise to plasmon excitations. In an ordinary metal the plasmon energy at $q = 0$ is of the order of several eV. However, in one-dimensional (and two-dimensional) systems this energy goes to zero as $q \to 0$. A low-energy-plasmon excitation is also possible even when the electrons are not one-dimensional. "Acoustic" plasmons with a frequency which goes to zero as $q \to 0$ may in principle exist in a three-dimensional multiband system, if there are two groups of electrons near the Fermi surface with widely different effective masses. These plasmons represent the movement of the two groups of electrons in opposite

directions without a net current. The properties of such plasmons and their possible existence in a V_3Ga crystal have been recently discussed by Gutfreund and Unna.[34] It follows from their estimates that the energy of the acoustic plasmon at $q = 0.02\pi/a$ is of the order of $\omega = 0.1$ meV. It is possible that the two phonon peaks observed in Nb_3Sn result from the interaction between a soft phonon and such a low-energy plasmon.

The present formalism is, in effect, a solution of Schrödinger's equation neglecting relaxation. From neutron and light scattering work on liquids and magnetic systems, we know that relaxation processes, heat diffusion, etc., have to be taken into account, and that a central peak is indeed observed in such systems with an amplitude proportional to $1 - c_v/c_p$. A central peak has also been observed in insulating solids near a second-order phase transition.[35] Because of these reasons, we face the following alternatives: (i) The central peak in Nb_3Sn is perhaps not due to electron-hole excitations at all. (ii) The central peak is due to electron-hole excitations, but the widths of the peaks may be narrower than calculated here, due to relaxation phenomena. Thus the question of the origin of the central peak in Nb_3Sn must be regarded as an open question as yet.

In view of the reservations raised so far, it is not clear how relevant is the simple model discussed in this paper to real β tungstens. However, we believe that the situation is quite different in the organic conductors mentioned in Sec. I. The one-dimensional character of the electron motion has been established quite reliably; there is only one family of parallel chains and the electron band structure is very simple. A superlattice with a wave vector $q = 2p_F$ was observed by Comes *et al.*[36] at room temperature in $K_2Pt(CN)_4Br_{0.3} \cdot 3H_2O$, by means of x-ray diffuse-scattering experiments. It was not clear whether this corresponds to a static Peierls deformation or a one-dimensional Kohn anomaly, as expected at temperatures above T_p. The latter was directly observed in these materials in recent coherent inelastic-neutron-scattering experiments.[21] More neutron-scattering experiments on these materials and on the TCNQ charge-transfer salts would be desired to study the details of the phonon dispersion around $2p_F$. In particular, one should look at line shapes in search for the two-branch structure predicted here. The knowledge of the phonon-excitation curve at $q = 2p_F$ is very important to the discussion of possible superconductivity in the TTF-TCNQ crystal. Some authors exclude the possibility of BCS-pairing,[37] because very soft phonons lead to an effective electron-electron repulsion. However, these authors do not take into account the higher branch, which does not go to zero even at $T = T_p$, and may provide sufficient effective attraction to make BCS pairing possible.

Recently, high superconducting transition temperatures were reported for Nb_3Ga,[38] Nb_3Ge[39] prepared very carefully. The question arises as to what degree of crystalline order is required in such compounds (as well as the better-known Nb_3Sn, Nb_3Al, V_3Si, V_3Ga, etc.[1]) to achieve a high value of T_c. (In V_3Au, a small degree of disorder is sufficient to destroy superconductivity,[40] but this material does not possess a high order of T_c to start with). In the spirit of the present work, we would attribute the high value of T_c to the Kohn anomaly,[16] and the length of an ordered linear chain needed to make use of this anomaly should be of order $l \sim 1/\Delta q$, where Δq is the width of the Kohn anomaly (Figs. 2 and 4). For the ideal linear chains considered in this work, $\Delta q/k_F \approx \hbar\omega_0/E_F$. For an electronic band with $E_F \approx 2$–3 eV (specifically, the $m_l = 0$ band[1]), we get $l \approx 50$. Barisic[5] considers another band, with a much smaller value of E_F, but also much smaller value of k_F and ω_0; thus for his bands, the value of l could be of a similar order. However, in realistic materials we have to allow for a band structure that is not ideally one dimensional, owing to next-nearest-neighbor transfer integrals, hybridization of bands, etc.[1] Thus, the width of the Kohn anomaly should in reality be determined by band-structure effects, and be much larger than $\hbar\omega_0/E_F$. Values of $\delta k_F/k_F \approx 0.1$–$0.2$ (Goldberg[41]) are likely, implying $l \approx 5$–10 atomic distances for the order required to achieve the high value of T_c.

ACKNOWLEDGMENTS

We benefited from correspondence with S. Barisic and discussions with J. Imry.

[1]For a recent review, see M. Weger and I. Goldberg, in *Solid State Physics*, edited by F. Seitz, D. Thurnbull and H. Ehrenreich (Academic, New York, 1973), Vol. 28, p. 1.

[2]M. Weger, Rev. Mod. Phys. 36, 175 (1964); J. Phys. Chem. Solids 31, 162 (1970).

[3]J. Labbe and F. Friedel, J. Phys. 27, 153 (1965); J. Phys. 27, 303 (1965).

[4]S. Berko and M. Weger, Phys. Rev. Lett. 24, 55 (1970); and in *Computational Physics* (Proceedings of the IBM Conference, Wildbad, 1971), edited by F. Herman (Plenum, New York, 1972).

[5]S. Barisic, Ann. Phys. (N. Y.) 7, 23 (1972).

[6]For a recent review, see I. F. Shchegolev, Phys. Status Solidi A 12, 9 (1972).

[7]S. Engelsberg and B. B. Varga, Phys. Rev. 136, A1582 (1964).

[8]A. M. Alfanas'ev and Yu. Kagan, Zh. Eksp. Teor. Fiz.

43, 1456 (1962) [Sov. Phys.-JETP 16, 1030 (1963)].
[9]R. E. Peierls, *Quantum Theory of Solids* (Oxford U. P., London, 1953), p. 108.
[10]H. Fröhlich, Proc. R. Soc. A 223, 296 (1954).
[11]B. Horovitz, H. Gutfreund, and M. Weger, Solid State Commun. 11, 1361 (1972).
[12]The Sawada method for the dense electron gas is described in R. Brout and P. Carruthers, *Lectures on the Many Electron Problem* (Interscience, New York, 1963), Sec. 3.2.
[13]S. Barisic, A. Bjelies, and K. Saub, Solid State Commun. 13, 1119 (1973).
[14]G. Shirane and J. D. Axe, Phys. Rev. Lett. 27, 1803 (1967).
[15]L. B. Coleman, M. J. Cohen, D. J. Sandman, F. G. Yamagishi, A. F. Garito, and A. J. Heeger, Solid State Commun. 12, 1125 (1973).
[16]H. Gutfreund, B. Horovitz, and M. Weger, J. Phys. C 7, 383 (1974); and Symposium on Superconductivity and Lattice Instabilities, Gatlinburg, Tenn., September 1973.
[17]J. Bardeen, Solid State Commun. 13, 357 (1973); and D. Allender, J. W. Bray, and J. Bardeen, Phys. Rev. B 9, 119 (1974).
[18]A. Suna (report of work prior to publication).
[19]M. J. Rice and S. Strassler, Solid State Commun. 13, 125 (1973); D. Bergmann and D. Rainer, Symposium on Superconductivity and Lattice Instabilities, Gatlinburg, Tenn., September 1973.
[20]A. Madhukar (report of work prior to publication).
[21]B. Renker, H. Rietschel, L. Pintschovins, W. Gläser, P. Bruesch, D. Kuse, and M. J. Rice, Phys. Rev. Lett. 30, 1144 (1973).
[22]W. L. McMillan, Phys. Rev. 167, 331 (1968).
[23]For example, A. L. Fetter and J. D. Walecka, *Quantum Theory of Many-Particle Systems* (McGraw-Hill, New York, 1971), Chaps. 5 and 9.
[24]G. Wentzel, Phys. Rev. 83, 163 (1951).
[25]A. Bychkov, L. P. Gorkov and I. E. Dzyaloshinsky, Zh. Eksp. Teor. Fiz. 50, 738 (1966) [Sov. Phys.-JETP 23, 489 (1966)].
[26]For example, J. R. Schrieffer, *Theory of Superconductivity* (Benjamin, New York, 1964), Sec. 5-8.
[27]C. G. Kuper, Proc. R. Soc. Lond. A227, 214 (1955).
[28]J. R. Schrieffer, in Ref. 26, Sec. 7-4.
[29]J. S. Shier and R. D. Taylor, Phys. Rev. 174, 346 (1968).
[30]L. R. Testardi, Phys. Rev. Lett. 31, 37 (1973).
[31]F. Y. Fradin, G. S. Knapp, and C. W. Kimball, Symposium on Superconductivity and Lattice Instabilities, Gatlinburg, Tenn., September 1973 .
[32]L. R. Testardi, in *Physical Acoustics*, edited by W. P. Mason and R. N. Thurston (Academic, New York, 1973) Vol. X.
[33]T. Maniv, J. Phys. Chem. Solids (to be published); Phys. Rev. Lett. 29, 584 (1972).
[34]H. Gutfreund and Y. Unna, J. Phys. Chem. Solids 34, 1523 (1973).
[35]R. Klein, Proceedings of Nato Study Institute—Anharmonic Lattices, Structural Transitions and Melting, April 1973, edited by T. Riste (unpublished), and references therein.
[36]R. Comes, M. Lambert, H. Lanois, and H. R. Zeller, Phys. Rev. B 8, 571 (1973).
[37]B. R. Patton and L. J. Sham, Phys. Rev. Lett. 31, 631 (1973).
[38]G. W. Webb, L. J. Vieland, R. E. Miller, and A. Wicklund, Solid State Commun. 9, 1969 (1971).
[39]J. R. Gavaler, in Ref. 31.
[40]J. Labbe and E. C. Van Reute, Phys. Rev. Lett. 24, 1232 (1970).
[41]I. B. Goldberg (unpublished).